Invited Talk on the Adriatico Research Conference:
"POLARIZATION DYNAMICS IN NUCLEAR AND PARTICLE PHYSICS",
Trieste (Italy) 7 to 10 January 1992

ELASTIC SCATTERING AND TOTAL CROSS SECTIONS OF POLARIZED NEUTRONS ON POLARIZED PROTONS AT SATURNE II

François Lehar
DAPNIA/SPP, CEN-Saclay, 91191 Gif sur Yvette, CEDEX, France

Abstract

Neutron-proton total cross section differences $\Delta\sigma_T$ and $\Delta\sigma_L$ as well as elastic scattering observables (including the differential cross sections), measured at SATURNE II, are presented. A major part of results was measured using the quasimonoenergetic polarized neutron beam and/or the polarized proton target. At several energies data are compared with measurements obtained in other laboratories. First direct reconstructions of the np scattering matrix at 0.84 and 0.88 GeV are shown.

1. Introduction

A large amount of new results for n-p elastic scattering and transmission experiments at intermediate energies appeared recently. A considerable part of them was measured at SATURNE II using the intense polarized beam of free neutrons obtained by a break-up of accelerated polarized deuterons. The total cross section differences $\Delta\sigma_T$ and $\Delta\sigma_L$ were measured in a large energy region[LEH87,FON91]. The elastic differential cross sections[WEL86,SIL89] and analyzing powers at small angles[KOR85,SIL89] were precisely determined. The analyzing power and spin correlations were measured either in quasielastic[BYS85,BAL87,LES88] or in elastic[BAL88] np scattering. Rescattering observables, including three spin-index parameters were determined using the Saclay frozen spin polarized proton target. Only a small part of data was published. The aim of SATURNE II measurements is a reconstruction of scattering matrix either via the phase shift analysis (PSA), or by a direct determination of scattering amplitudes.

In the present talk are mainly reported the results of two groups: I. "IKAR COLLABORATION" and II. "NUCLEON-NUCLEON GROUP". In both groups participated, fully or partially, physicists from differents laboratories. All their names in the IKAR collaboration as well as theirs, participating on unpublished results of the NN Group, are listed in an alphabetic order :

I. A.V.Dobrovolsky, A.V.Khanzadeev, G.A.Korolev, J.C.Lugol, D.E.Petrov, J.Saudinos, B.H.Silverman, E.M.Spiridenkov, Y.Terrien, A.A.Vorobyov and F.Wellers.

II. P.Bach, J.Ball, L.S.Barabash, J.Bystricky, P.Chaumette, P.Chesny, M.Combet, P.Demierre, J.Deregel, J.M.Fontaine, G.Gaillard, J.P.Goudour, R.Hess, Z.Janout, B.A.Khachaturov, A.Klett, R.Kunne, C.D.Lac, F.Lehar, A. de Lesquen, D.Lopiano, M. de Mali, A.Nakach, F.Perrot-Kunne, R.Peschina, D.Rapin, E.Rossle, L. van Rossum, H.Schmitt, J.L.Sans, P.Sormani, H.Spinka and Yu.A.Usov.

In the present talk, the notation of observables and the scattering amplitude representation as in ref.[BYS79] are used.

2. Polarized Beam and Polarized Target

A small part of n-p data was measured with a polarized deuteron beam considered as a beam of quasifree protons and neutrons. For such a beam the polarizations of protons and neutrons in accelerated deuterons are equal and the ratio of the quasielastic pp to np asymmetries is independent on the deuteron beam polarization.

Using the NN polarimeter and assuming that the quasielastic pp analyzing power is the same as that one for pp elastic scattering, one can determine the polarization of the proton and neutrons in the deuterons. It is equal to 0.5773 ± 0.003 (the error is statistical only) and it was found to be independent on the deuteron beam energy[BYS85]. This is in agreement with an absence of any deuteron depolarizing resonance at SATURNE II. The proton and neutron polarizations agree with the measurement of the deuteron beam polarization, measured downstream the ion source at very low energy.

The angular dependence of several observables (A_{oono}, A_{oonn}, A_{oosk}) in quasifree pp scattering agrees with the fit of free pp data and one can assume that this also holds for np scattering.

At SATURNE II, "break up" free neutron beams were first built for the IKAR experiment[KOR85,SIL89] and later for the Nucleon-Nucleon (NN) program[LEH87]. The characteristics of both beams are similar. Vector-polarized deuterons are broken up on a 20 cm thick Be target. For the NN beam line[LEH87,BAL87] break-up protons are swept away by a magnetic field while the remaining neutron beam is allowed to pass through a spin-rotating solenoid and precessing magnets. This allows to the neutron polarization to be oriented along any of the three orthogonal directions, $\vec{n}$ (vertical), $\vec{s}$ (side-way) and $\vec{k}$ (longitudinal). The neutron beam is defined by 8 meters of collimators inserted into the 17.5 m long neutron beam line. The beam spot at the target is either 20 mm or 30 mm in diameter. The MIMAS booster, recently put into operation, has allowed an increase the SATURNE II polarized

deuteron beam intensity up to 3.10^{11} deuterons/spill providing up to 10^7 neutrons/spill/cm^2 on the target.

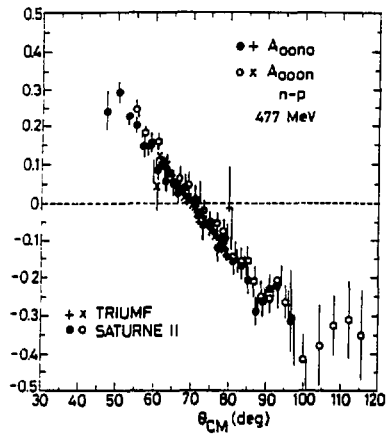

Fig. 1 Angular dependence of the beam and target analyzing powers at 477 MeV.
● ..... A_{oono} SATURNE II
\+ ..... A_{oono} ref.[BAN89]
o ..... A_{ooon} SATURNE II
x ..... A_{ooon} [BAN89]

A.Boudard and C.Wilkin [BOU87] calculated the polarization of the "break-up" neutrons in the forward direction, using the results from refs[ARV84,ARV88,BYS85C]. They predicted a value of 0.59 at SATURNE II. Experimentally it can be obtained by comparing the beam analyzing power A_{oono} and the target analyzing power A_{ooon}, measured with a polarized neutron beam and unpolarized proton target and vice versa. The slope of the angular dependence of A_{oono} near the zero-crossing point must be equal to that of A_{ooon}, which is independent of the beam polarization. The comparison was done at 477 MeV, i.e. at the very energy where a precise test of isospin invariance ($A_{oono}(np) = A_{ooon}(np)$) has been done at TRIUMF[BAN89]. Both TRIUMF and SATURNE II results are shown in Fig. 1. This comparison gives 0.59 ± 0.02 for the "break-up" neutron beam polarization (in perfect agreement with the calculations[BOU87]).

The neutron beam enters in the 35 mm thick, 40 mm wide and 49 mm high PPT [BER86]. The target materiel was pentanol, with a typical proton polarization of 85%. The relaxation time of the target was ~ 30 days at 38 mK in a holding field of 0.33 Tesla. The PPT polarization may be also oriented in any of the $\vec{n}$, $\vec{s}$ or $\vec{k}$ directions (only the vertical and longitudinal target spin directions were employed). The experiments using an incident deuteron beam were done with the PPT 44 mm long and 2 cm in diameter.

3. Total Cross Section Differences for np Scattering

The np total cross differences $\Delta\sigma_T(np)$ and $\Delta\sigma_L(np)$, using free polarized neutrons, were measured for the first time at SATURNE II. Four points with

relatively large errors were published[LEH87]. These results were completed by new measurements at 9 to 10 energies for each observable[FON91]. The total cross section differences were measured simultaneously with other spin-dependent np elastic scattering observables.

The experimental set-up and its electronics were described in refs[LEH87,FON91]. The beam monitor S and the transmission detector T were of similar design. The 40 to 60 mm thick CH_2 convertors are placed immediately after large veto scintillators, and charged particles emitted forward are detected by two counters in coincidence. Compared to the live-target method this array is less efficient but provides better stability of detection efficiency since the pulse height distribution is peaked far above the discriminator threshold. Note that only stability is important. The results depend neither on the absolute efficiencies of S and T nor on their ratio. On the other hand the detection efficiency must be independent of the neutron polarization. The solid angle subtended by the transmission detector at the center of the target could was Ω = 2.5 msr. for most of measurements. One estimates that the difference between the measured value $\Delta\sigma_L$ and the extrapolated value $\Delta\sigma(\Omega=0°)$ is less than 0.05 mb. This is smaller than the experimental errors in the experiment. The effects due to misalignment and tranverse beam polarization cancel when taking the simple average between measurements with opposite target polarizations[PER86]. For example a test with s-type beam and k-type target at 0.84 GeV gives (0.12 ± 0.74)mb.

The Saclay results were soon followed by PSI measurements in the energy region from 140 to 590 MeV. The latter used a similar counter set-up, but completely different electronics. A polarized neutron beam with a continuous energy spectrum[BIN89] was used so that $\Delta\sigma_T$ or $\Delta\sigma_L$ data could be collected simultaneously over the entire energy range 140 - 590 MeV[BIN91].

The observable $\Delta\sigma_L$ has also been measured at five energies at LAMPF[BED91]. The measurements were done with a quasi-monoenergetic polarized neutron beam produced in pd → n + X scattering of longitudinally polarized protons. A large neutron counter hodoscope had to be used because of the small neutron beam intensity. Figs 2a,b show the energy dependence of all these measurements for σ_{1tot}(np) and $-\Delta\sigma_L$(np), respectively. One can notice an excellent agreement between all data sets. A dip at ~ 600 MeV for both observables is less pronounced than in the analogous pp quantities. A very broad maximum can be observed at ~ 0.9 GeV in $-\Delta\sigma_L$ energy dependence.

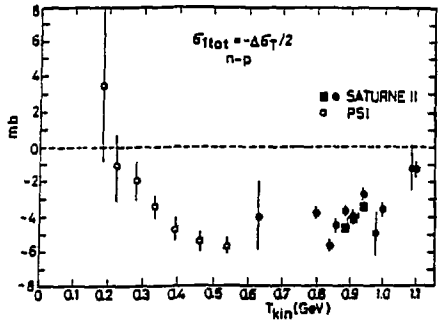

Fig. 2a σ_{1tot} energy dependence.

● ..... SATURNE II [FON91]
○ ..... PSI [BIN91]

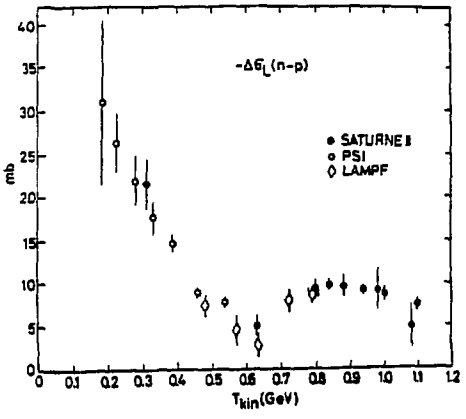

Fig. 2b $-\Delta\sigma_L$ energy dependence.

● ..... SATURNE II [FON91]
○ ..... PSI [BIN91]
Diamonds ..... LAMPF [BED91]

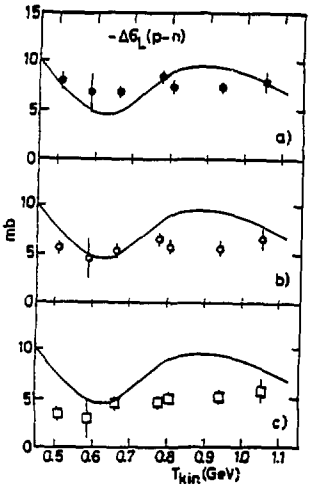

Fig. 3 Free np $-\Delta\sigma_L$ energy dependence compared with the ANL-ZGS quasi-elastic transmission measurements.

Full line ..... handdrawn energy dependence for free np transmission
Full dots (Fig 3a) ..... uncorrected data[AUE81]
Open circles (Fig. 3b) .. ANL corrections[ARG87]
Open squares (Fig. 3c) .. corrections from ref.[KRO82].

In fact, the first $\Delta\sigma_L$ results were obtained in 1981 in a quasifree p-n transmission measurement at the ANL-ZGS[AUE81]. This experiment measured $\Delta\sigma_L$(pd) and $\Delta\sigma_L$(pp) by transmission of polarized protons through a partially deuterated polarized target. Taking a simple difference between pd and pp results, corrected only for beam and target polarizations and for Coulomb-Nuclear rescattering including deuteron break-up, yields data in fairly good agreement with the Saclay, PSI and LAMPF results. This is demonstrated in Fig. 3a where the full line represents the hand drawn energy dependence of $-\Delta\sigma_L$ and the black dots are the

"uncorrected" ANL-ZGS results. The data corrected for Glauber-type rescattering[ARG87] are presented in Fig 3b by open circles. Between 0.8 and 1.1 GeV these results disagree with the free np results. In 1982 the ANL-ZGS data were corrected by Kroll[KRO82] for Glauber-type rescattering including final 3-body state interactions[GRE82] (open squares). This correction increases the disagreement as can be seen in Fig. 3c (open squares).

In the past no serious difference has ever been was found between elastic and quasielastic scattering observables and that all attempts to correct quasifree scattering have failed. Let me mention a result obtained at PSI[BIN89] which is relevant to this problem. It was found that the polarization transfer parameters $K_{ok"ko}$ and K_{onno} for the pC → n + X reaction at angles close to 180° CM have practically the same energy dependences as the observables for free np scattering.

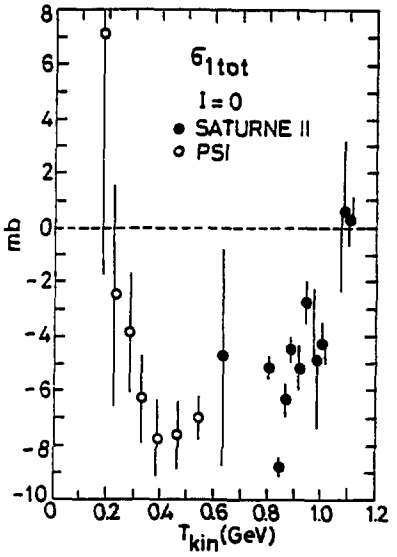

Fig. 4a Energy dependence of σ_{1tot} for the I=0 state.
Statistical errors are shown.
○ ..... PSI [BIN91]
● ..... SATURNE II [FON91]

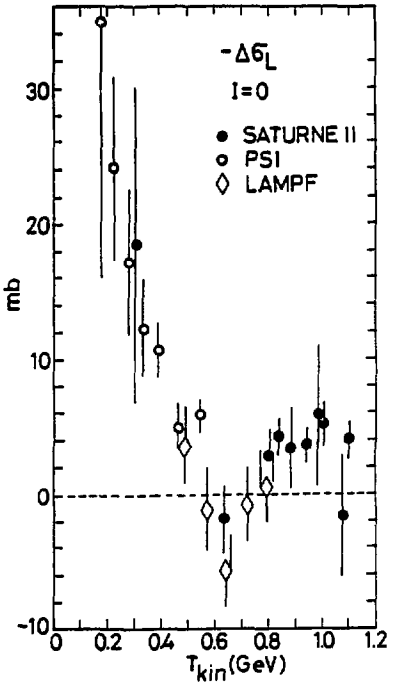

Fig. 4b Energy dependence of $-\Delta\sigma_L$ for I=0 state.
Statistical errors are shown.
○ ..... PSI [BIN91]
Diamonds ..... LAMPF [BED91]
● ..... SATURNE II [FON91]

4. Isospin I=0 Total Cross Sections

From the measured σ_{0tot}, $\Delta\sigma_T$ and $\Delta\sigma_L$ for pp and np scattering, it is possible to determine the I=0 total cross sections. Since the corresponding pp observables are known, the np quantities presented above were used for these calculations. Figs 4a and 4b show the energy behavior of $\sigma_{1tot}(I=0)$ and $-\Delta\sigma_L(I=0)$, respectively. The shape of σ_{1tot} and $-\Delta\sigma_L$ observables for I=0 state is similar to the one observed for the corresponding np observables. A dip at ~ 0.6 GeV is well pronounced also in the energy dependence of pp quantities. In the past this dip was attributed to a possible resonance in the $^1D_2$ partial wave, but this wave is absent in I=0 amplitudes. Therefore one cannot say that the energy dependence of I=0 observables support the hypothesis attributing the origin of the σ_{1tot} and $-\Delta\sigma_L$ behavior in pp and np scattering only to the $^1D_2$ partial wave.

5. Differential Cross Sections for Elastic np Scattering

Differential cross sections at medium and large scattering angles have been accurately measured for many years now in different laboratories. Measurements at small angles, however, have been scarce. At SATURNE II, the small angle elastic np differential cross section at 378, 481, 532, 582, 633, 683, 708, 784, 834, 884, 934, 985, 1085 and 1135 MeV was measured by Saclay and Gatchina groups[SIL89], resulting in 585 experimental points. A selective choice of results at 6 energies is shown in Figs 5a,b. In these experiments, neutrons were scattered at small angles inside a high-pressure drift chamber IKAR which measured the slow recoil proton angle and path length in the gas. For A_{oono} measurements at small angles (see next

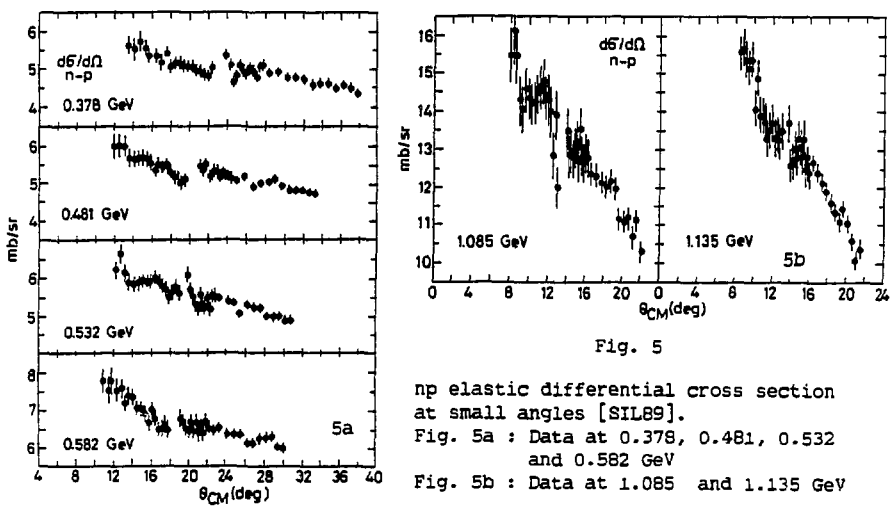

Fig. 5

np elastic differential cross section at small angles [SIL89].
Fig. 5a : Data at 0.378, 0.481, 0.532 and 0.582 GeV
Fig. 5b : Data at 1.085 and 1.135 GeV

Section) the experimental set-up was completed by two large neutron counters in order to determine the left-right asymmetry. These measurements were performed at 0.633, 0.784, 0.834, 0.934 and 0.985 GeV[KOR85,SIL89].

6. Spin Dependent Observables.

In the Nucleon-Nucleon program at SATURNE II were measured 11 spin dependent *np observables* at 840, 880, 940, 1000 and 1100 MeV, in order to determine directly the np scattering amplitudes. They are listed in Table 1. Some dedicated measurements were also performed at other energies.

Table 1 - np Observables measured in the NN program at SATURNE II

Orientation of Polarizations	Beam / Target	$\pm \vec{k}$ / $\pm \vec{k}$	$\pm \vec{n}$ / $\pm \vec{n}$	$\pm \vec{s}$ / $\pm \vec{k}$
Rescattering Observables	3-index	N_{onkk}	N_{onnn}	N_{onsk}
	2-index	$D_{os"ok}$ $K_{os"ko}$	D_{onon} K_{onno}	$D_{os"ok}$ $K_{os"so}$
	1-index	P_{onoo}	P_{onoo}	P_{onoo}
No Rescattering	2-index	A_{ookk}	A_{oonn}	A_{oosk}
	1-index		A_{oono} A_{ooon}	
Transmission		$\Delta\sigma_L$	$\Delta\sigma_T$	

The two arm spectrometer comprizing trigger counters and hodoscopes, 8 MWPC's and an analyzing magnet was used. Neutrons scattered at angles <90° CM were detected in a large neutron counter hodoscope having a detection efficiency of 0.2 and the angular resolution ±0.22° lab. horizontally and ±0.35° vertically. Transverse components of recoil proton polarization were determined by rescattering on a carbon analyzer 5 to 6 cm thick. Neutrons scattered at large angles may also be converted into charged particles on the same block. For these events the detection efficiency is is considerably smaller.

In order to correctly monitor measurements with two opposite target polarization directions, a CH_2 target 3 to 10 mm thick was positionned downstream from the PPT. Particles scattered either on PPT or on the CH_2 target produce independent triggers, but all tracks are detected in the same MWPC's. Statistics of events from CH_2 target, is used for the normalization of statistics from PPT.

Approximately one third of recorded data was analyzed. In Fig. 6a,b,c are shown the results of the beam and target analyzing powers A_{oono} and A_{ooon} measured with

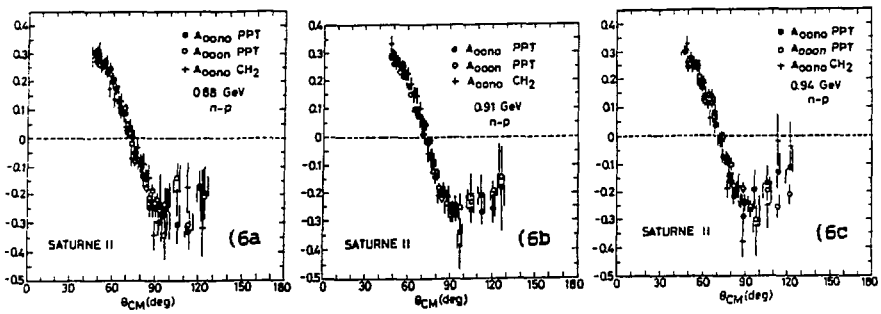

Fig. 6 Analyzing powers at 0.88 GeV (6a), 0.91 GeV (6b) and 0.94 GeV (6c). A_{oono} (•) and A_{ooon} (o) are measured with PPT, and A_{oono} (+) is measured with the CH_2 target.

the PPT and those of A_{oono}, measured using the CH_2 target. Figs 7a to 7c compare different elastic and quasielastic[BYS85,BAL87] A_{oono} data measured at SATURNE II, including the IKAR measurements[KOR85,SIL89]. All results are in an excellent agreement. The data at large angles are measured using the neutron charge exchange on the carbon block and their errors are large.

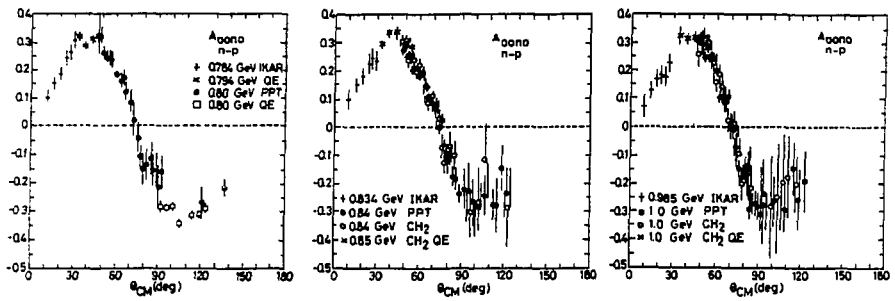

Fig. 7 The beam analyzing power A_{oono} around 0.80 GeV (7a), 0.84 GeV (7b) and 1 GeV (7c). Symbols : + ... [KOR85], x ... [BYS85], • ... NN group PPT o ..... CH_2, squares .. [BAL87], QE ..... d beam

Fig. 8 show the angular dependence of the spin correlation A_{oonn} between 0.8 and 1.1 GeV. This observable change considerably its shape above 0.84 GeV. Around 0.8 GeV the elastic and quasielastic [LES88] SATURNE II results are compared with the LAMPF data [NAT89]. The spin correlations A_{ookk} and A_{oosk} are plotted in Figs 9 and 10, respectively. The SATURNE II data at 0.84 GeV are compared with the LAMPF measurements at 0.788 GeV[GAR89].

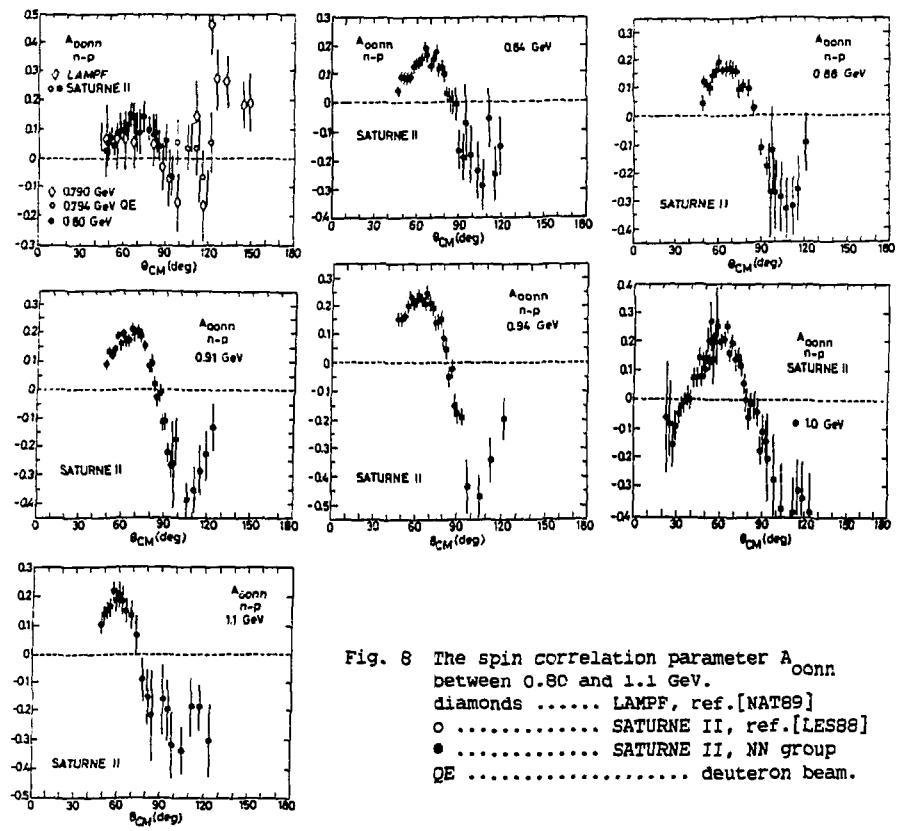

Fig. 8 The spin correlation parameter A_{oonn} between 0.80 and 1.1 GeV.
diamonds ..... LAMPF, ref.[NAT89]
o ..... SATURNE II, ref.[LES88]
● ..... SATURNE II, NN group
QE ..... deuteron beam.

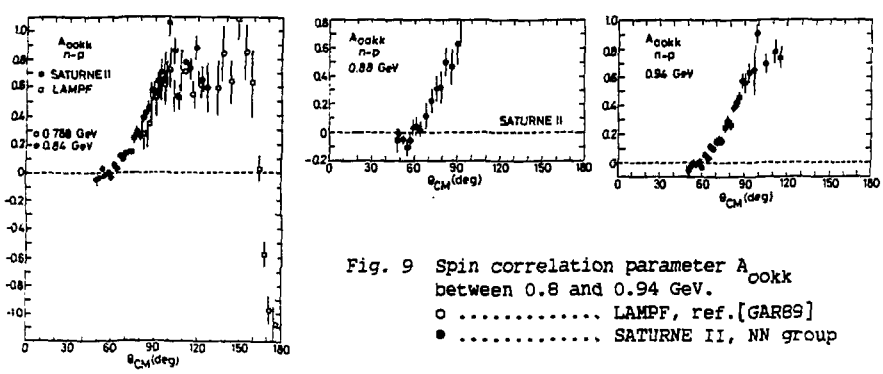

Fig. 9 Spin correlation parameter A_{ookk} between 0.8 and 0.94 GeV.
o ..... LAMPF, ref.[GAR89]
● ..... SATURNE II, NN group

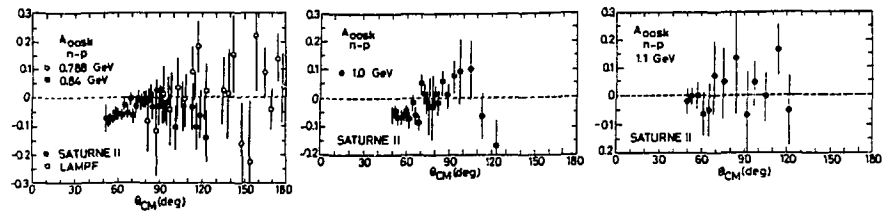

Fig. 10 Spin correlation parameter A_{oosk} between 0.8 and 1.1 GeV.
o ..... LAMPF, refs[GAR89]
• ..... SATURNE II, NN group

The rescattering observables D_{onon} and K_{onno} at three energies are shown in Fig.11. At 0.91 GeV are compared the results from all analyzed data (open circles) with the results from one run (black dots). Preliminary SATURNE II results for $K_{os"so}$ and $K_{os"ko}$ at 0.84 GeV (black dots) are compared with LAMPF data [MNA91] at 0.788 GeV (open circles) in Figs 12 and 13, respectively. The rescattering observables, including the three-spin index quantities were analyzed at few energies only and the errors are still large.

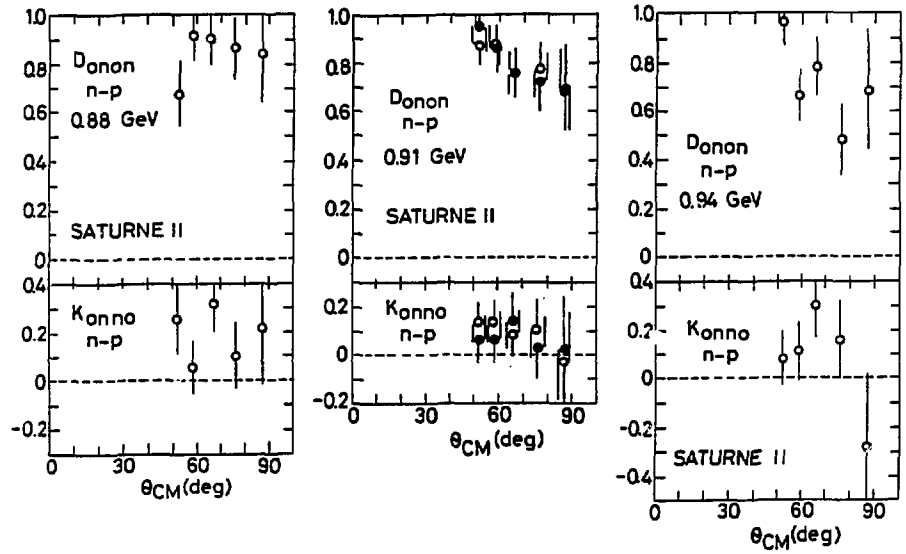

Fig. 11 The rescattering observables D_{onon} and K_{onno} at three energies. At 0.91 GeV are compared the results from all analyzed data (open circles) with the results from one run (black dots).

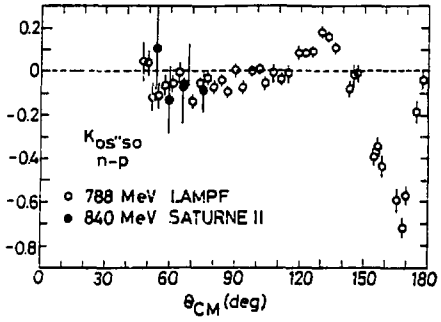

Fig. 12 The rescattering observable $K_{os"so}$ around 0.8 GeV.
o ..... LAMPF ref. [MNA91]
• ..... SATURNE II, NN group.

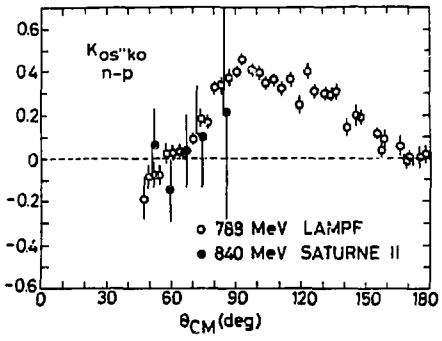

Fig. 13 The rescattering observable $K_{os"ko}$ around 0.8 GeV.
o ..... LAMPF ref. [MNA91]
• ..... SATURNE II, NN group.

6. I=0 and I=1 Amplitudes in the Forward Direction

At zero degree, there remain only 3 independent complex scattering amplitudes therefore at least 6 independent experimental quantities are required to directly compute the amplitudes. But only three total cross sections, σ_{0tot} $\Delta\sigma_T$, $\Delta\sigma_L$ can be measured at 0°. (Recall that the invariant amplitude representation [BYS79] is used in the present paper). Optical theorems give access to the imaginary parts

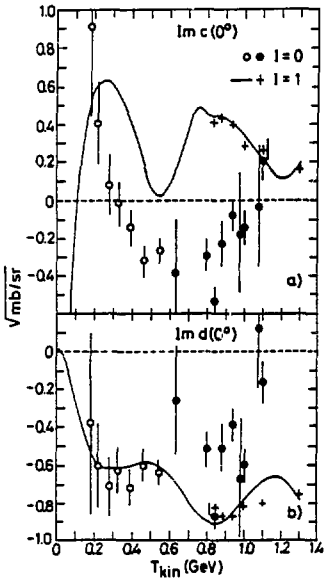

Fig. 14 – Energy dependence of the imaginary parts of amplitudes c (Fig. 14a) and d (Fig. 14b) at 0° for I = 0 and I = 1 isospin states ($\sqrt{mb/sr}$ units). Statistical errors are shown.
o ..... PSI, ref.[BIN91]
• ..... SATURNE II [FON91]
+ ..... PSA Saclay-Geneva, [BYS90]
Solid line .... PSA Saclay-Geneva, [BYS87,LEH87A].

of (a + b), c and d via measurements of σ_{0tot} $\Delta\sigma_T$, $\Delta\sigma_L$. Using the relation Amp(I=0) = 2Amp(np) - Amp(pp) one can extract separately the amplitudes for each isospin state. This is shown in Figs 14a,b for the amplitudes Im c and Im d, respectively. The energy dependence for I=0 parts was calculated from the data [BIN91,FON91] and that for I=1 imaginary parts from the Saclay-Geneva phase shift analyses [BYS87,BYS90,LEH87A].

7. Amplitude Analysis of np Elastic Scattering

In Table 1 were shown available linearly independent observables. In the present at three angles (approximately 54°, 61° and 73°) the analysis provide 11 spin observables at 0.84 and 0.88 GeV. Using, in addition, the known elastic np differential cross sections[BYS78,BYS80], one has complete sets, which allow the direct reconstructions of the scattering matrix. These reconstructions are shown in Figs 15 and 16, where are plotted absolute values and relative phases of invariant amplitudes a,b,c,d and e (φ_e=0, Re e =|e|)[BYS79]. Three to four solu-

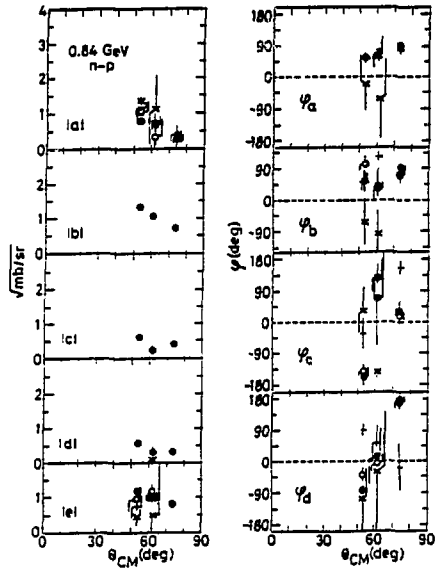

Fig. 15 Direct reconstruction of the np scattering matrix at 0.84 GeV. Absolute values and relative phases of invariant amplitudes a to e at three scattering angles are shown. The solutions denoted by •, o and + symbols have an equal statistical probability, solution (x) is less probable.

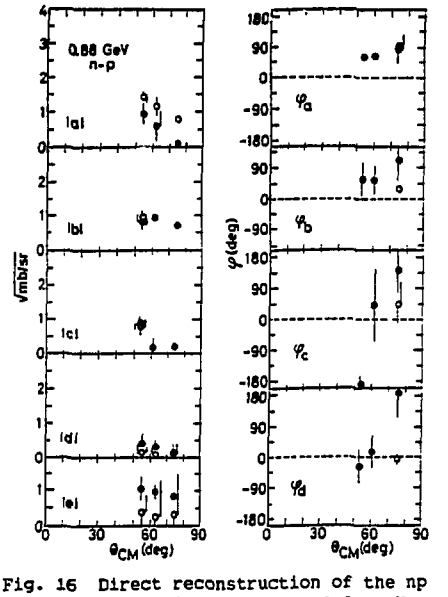

Fig. 16 Direct reconstruction of the np scattering matrix at 0.88 GeV. Absolute values and relative phases of invariant amplitudes a to e at three scattering angles are shown. The solutions denoted by • and o symbols have the same statistical probability.

tions, were found at 0.84 GeV, two of them (• and o) are similar and one (x) is less probable. Two solutions are plotted at 0.88 GeV, where the input data errors are larger than at 0.84 GeV. The solution denoted by "o" at 54° and 61° CM gives the errors of relative phases larger than ±180° and only the absolute values are plotted. At ~73°, close to the zero-crossing point, a third "degenerated" solution (Im a = 0) with small χ^2 exists, but is not plotted here. There is an excellent agreement between the reconstructions at the two energies. The authors of the reconstruction (in the alphabetic order) are:

P.Bach, J.Ball, R.Binz, J.Bystricky, J.M.Fontaine, G.Gaillard, J.P.Goudour, R.Hess, A.Klett, R.Kunne, C.D.Lac, F.Lehar, A. de Lesquen, M. de Mali, F.Perrot, R.Peschina, D.Rapin, E.Rossle, L. van Rossum, H.Schmitt and P.Sormani.

The preliminary results shown here represent the first numerical amplitude analyses for the np system. It remains uncertain whether the accuracy of some observables will be sufficient or not for an unique solution at all energies.

8. CONCLUSIONS

One cannot say that at intermediate energies exist enough of np elastic scattering data for a "good" PSA or an amplitude analysis solution. Even for the spin independent observables there is a lack of total inelastic or total elastic np cross sections, the reaction np → npπ^o remains badly determined and the differential np cross section between 30° and 130° CM above 0.8 GeV are rare. Measurements at SATURNE II will considerably affect the word data bank and give a possibility to correctly extend the PSA up to 1.1. GeV. The results allowed, for the first time, the direct reconstructions of the np scattering matrix.

Nevertheless new data are needed and well selected nucleon-nucleon experiments at any energy will improve our knowledge NN interactions. This concerns all existing accelerators, without any exception. Structures in NN scattering must be studied not only on the basis of the energy and angular dependences of observables, but also on the basis of scattering amplitudes (if it will be possible). In this case the number of suggested dibaryonic resonances may be considerably reduced.

Group, are listed in an alphabetic order :

References

ARG87 Argonne Private Communication, July 1987
ARV84 J.Arvieux et al., Nucl.Phys. A431 (1984)
ARV88 J.Arvieux et al., Nucl.Instr.Methods A273 (1988) 48
AUE81 I.P.Auer et al., Phys.Rev.Lett. 46 (1981) 1177
BAL87 J.Ball et al., Nucl.Phys. B286 (1987) 635
BAL88 J.Ball et al., Z.Phys.C 40 (1988) 193
BAN89 D.Bandyopadhyay et al., Phys.Rev. C40 (1989) 2684
BED91 M.Beddo et al., Phys.Lett. 25B (1991) 24
BER86 R.Bernard et al. Nucl.Instr.Methods A249 (1986) 176
BIN89 R.Binz et al., Phys.Lett. B231 (1989) 323
BIN91 R.Binz et al., To be published in Nucl.Phys. A
BOU87 A.Boudard and C.Wilkin, Private Communication 1987.
BYS78 J.Bystricky and F.Lehar, Physics Data Nr. 11-1, part I and II (1978), Nr 11-2 and 11-3 (1981) ed. H.Behrens and G.Ebel (Fachinformationszentrum Karlsruhe)
BYS79 J.Bystricky, F.Lehar and P.Winternitz, J.Physique (Paris) 39 (1979) 1
BYS80 J.Bystricky et al., Landolt-Bornstein Tables, New Series, Vol. 9a, (1980), ed. H.Schopper (Springer Verlag)
BYS85 J.Bystricky et al., Nucl.Phys. A444 (1985) 597
BYS87 J.Bystricky et al., J.Physique France 48 (1987) 199
BYS90 J.Bystricky et al., J.Physique France 51 (1990) 2747
FON91 J.M.Fontaine et al., Nucl.Phys. B358 (1991) 297
GAR89 R.W.Garnett et al., Phys.Rev. D40 (1989) 1708
GRE82 W.Grein and P.Kroll, Nucl.Phys. A377 (1982) 505
KOR85 G.A.Korolev et al., Phys.Lett. B165 (1985) 262
KRO82 P.Kroll, Private Communication, September 20, 1982
LEH87 F.Lehar et al. Phys.Lett. B189 (1987) 341
LEH87A F.Lehar et al., J.Physique France 48 (1987) 1273
LES88 A. de Lesquen et al., Nucl.Phys. B304 (1988) 673
MNA91 M.W.McNaughton et al., to be published in Phys.Rev. C
NAT89 S.Nath et al., Phys.Rev. B39 (1989) 3520
PER86 F.Perrot et al., Nucl.Phys. B278 (1986) 881
SIL89 B.H.Silvermann et al., Nucl.Phys. A499 (1989) 763
WEL86 F.Wellers, Thesis, Orsay, January 9, 1986